Ultra High Energy Cosmic Rays

Todor Stanev
Bartol Research Institute, University of Delaware, Newark, DE 19716

We discuss theoretical issues and experimental data that brought the ultra high energy cosmic rays in the list of Nature's greatest puzzles. After many years of research we still do not know how astrophysical acceleration processes can reach energies exceeding 10^{11} GeV. The main alternative *top-down* mechanism postulates the existence of super massive X-particles that create a particle spectrum extending down to the observed energy through their decay channels. The propagation of nuclei and photons from their sources to us adds to the puzzle as all particles of these energies interact with the ambient photons, mostly of the microwave background. We also describe briefly the main observational results and give some information on the new experiments that are being built and designed now.

1. INTRODUCTION

More than forty years ago, in 1963, John Linsley [1] published an article about the detection of a cosmic ray of energy 10^{20} eV. The article did not go unnoticed, neither it provoked many comments. The few physicists that were interested in high energy cosmic rays were then convinced that the cosmic ray energy spectrum can continue forever. The fact that cosmic rays may have energies exceeding 10^6 GeV (10^{15} eV) was established in the late thirties by Pierre Auger and his collaborators. Showers of higher and higher energy were detected in the mean time - seeing a 10^{20} eV shower seem to be only a matter of time and exposure. Already in the fifties there was a discussion about the origin of such ultra high energy cosmic rays (UHECR) and Cocconi [2] reached the conclusion that they must be of extragalactic origin since the galactic cosmic rays are not strong enough contain such particles.

How exclusive this event is became obvious three years later, after the discovery of the microwave background. Almost simultaneously Greisen in US [3] and Zatsepin&Kuzmin [4] in the USSR published papers discussing the propagation of ultra high energy particles in extragalactic space. They calculated the energy loss distance of nucleons interacting in the microwave background and reached the conclusion that it is shorter than the distances between powerful galaxies. The cosmic ray spectrum should thus have an end around energy of 5×10^{19} eV. This effect is now known as the GZK cutoff.

The experimental statistics of such event grew with years, although not very fast. The flux of UHECR of energy above 10^{20} eV is estimated to 0.5 to 1 event per square kilometer per century per steradian. Even big detectors of area tens of km^2 would only detect few events for ten years of work. The topic became one of common interest during the last decade of the last century when ideas appeared for construction of detectors with effective areas in thousand of km^2. Such detectors would detect tens of events per year and finally solve all mysteries surrounding UHECR, which I will attempt to convey to you.

Cosmic rays are usually defined as charged nuclei that originate outside the solar system. They come on a featureless, power law like, $F(E) = K \times E^{-\alpha}$, spectrum that extends beyond 10^{11} GeV per particle, as shown above 100 GeV in Fig. 1. There are only two distinct features in the whole spectrum. At energy above 10^6 GeV the power law index α steepens from 2.7 to about 3.1. This is called *the knee* of the cosmic ray spectrum. At energy above 10^9 GeV the spectrum flattens again at *the ankle*. Both energy ranges, which are still not very well measured are indicated in the figure.

The common wisdom is that cosmic rays below the knee are accelerated at galactic supernovae remnants. Cosmic rays above the knee are also thought to be of galactic origin, although there is no clue of their acceleration sites. Cosmic rays above the ankle are thought to be extragalactic. When the total energy range is included the flux of cosmic rays varies by more than 30 orders of magnitude. Note that Fig. 1 shows EdF/dE and its slope is $\gamma = \alpha - 1$. The numbers of the left hand side of the figure shows the flux of cosmic rays in 'natural' units. It is obvious that direct experiments for cosmic ray detection, that are flown in satellites or balloons, can not carry forever because of

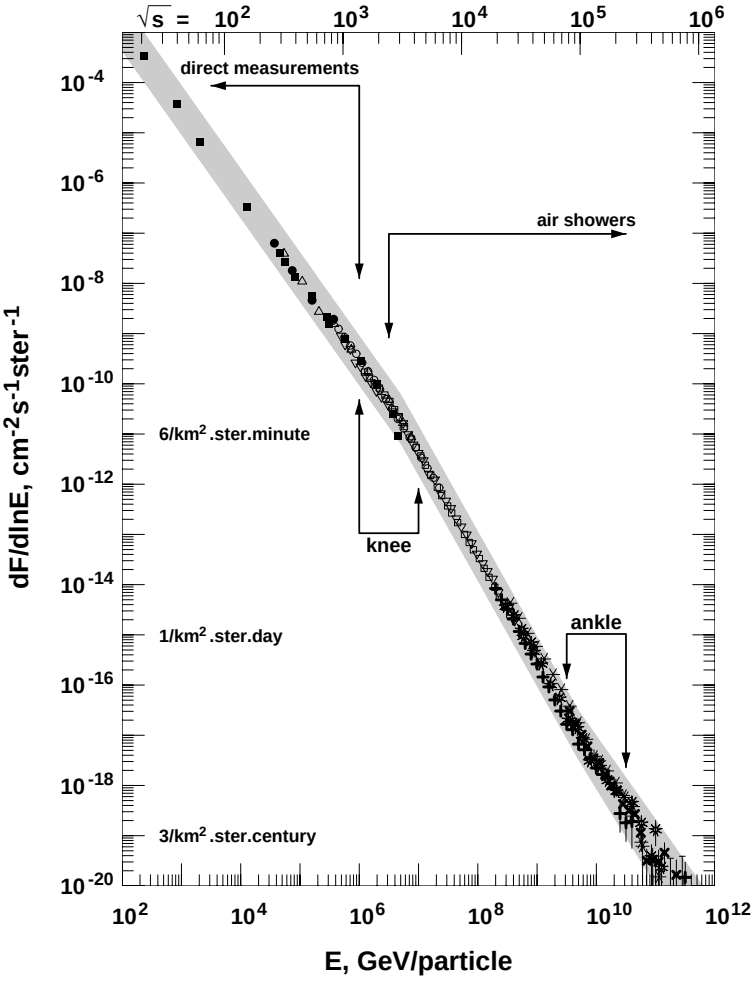

Figure 1: Energy spectrum of the cosmic ray nuclei.

statistical limitations. Some data from direct measurements are plotted with full symbols. All other symbols come from air shower measurements.

1.1. Air Shower Detection Methods.

Cosmic rays of energy above 10^{14} eV are detected by the showers they generate in the atmosphere. The atmosphere contains more than ten interaction lengths even in vertical direction and is much deeper for particles that enter it under higher zenith angles. It is thus a deep calorimeter in which the showers develop, reach their maximum, and then start being absorbed. There are generally two types of air shower detectors: air shower arrays and optical detectors. Air shower arrays consist of a large number of particle detectors that cover large area. The shower triggers the array by coincidental hits in many detectors. The most numerous particles in an air shower are electrons, positrons and photons. The shower also contains muons, that are about 10% of all shower particles, and hadrons (see the lecture of G. Schatz for more information).

The direction of the primary particle can be reconstructed quite well from the timing of the different hits, but the shower energy requires extensive Monte Carlo work with hadronic interaction models that are extended orders of magnitude above the accelerator energy range. The type of the primary particles can only be studied in statistically big samples because of the fluctuations in the individual shower development. Even then it is strongly affected by the differences in the hadronic interaction models.

The optical method uses the fact that part of the particle ionization loss is in the form of visible light. All charged particles emit in air Cherenkov light in a narrow cone around their direction. In addition to that charged particles excite Nitrogen atoms in the atmosphere, which emit fluorescence light. The output is not large, about 4 photons per meter, but the number of shower particles in UHECR showers is very large, and the shower can be seen from distances exceeding 30 km. The fluorescence detection is very suitable for UHECR showers because the light is emitted isotropically and can be detected independently of the shower direction. Since optical detectors follow the shower track, the direction of the primary cosmic ray is also relatively easy. The energy of the primary particles is deduced from the total number of particles in the shower development, or from the number of particles at shower maximum. The rough number is that every particle at maximum carries about 1.5 GeV of primary energy. The mass of the primary cosmic ray nucleus is studied by the depth of shower maximum X_{max}, which is proportional to the logarithm of the primary energy per nucleon while the total energy depends on the number of particles at maximum.

1.2. The Highest Energy Cosmic Ray Event

The highest energy cosmic ray particle was detected by the Fly's Eye experiment [5]. We will briefly describe this event to give the reader an idea about these giant air showers. The energy of the shower is estimated to be 3×10^{20} eV. This is an enormous macroscopic energy. 10^{20} eV is equivalent to 1.6×10^{8} erg, 2.4×10^{34} Hz and the energy of 170 km/h tennis ball. Fly's Eye was the first air fluorescence experiment, located in the state of Utah, U.S.A. Fig. 2 shows the shower profile of this event as measured by the Fly's Eye in the left hand panel. Note that the maximum of this shower contains more than 2×10^{11} electrons and positrons. Both the integral of this shower profile and the number of particles at maximum give about the same energy.

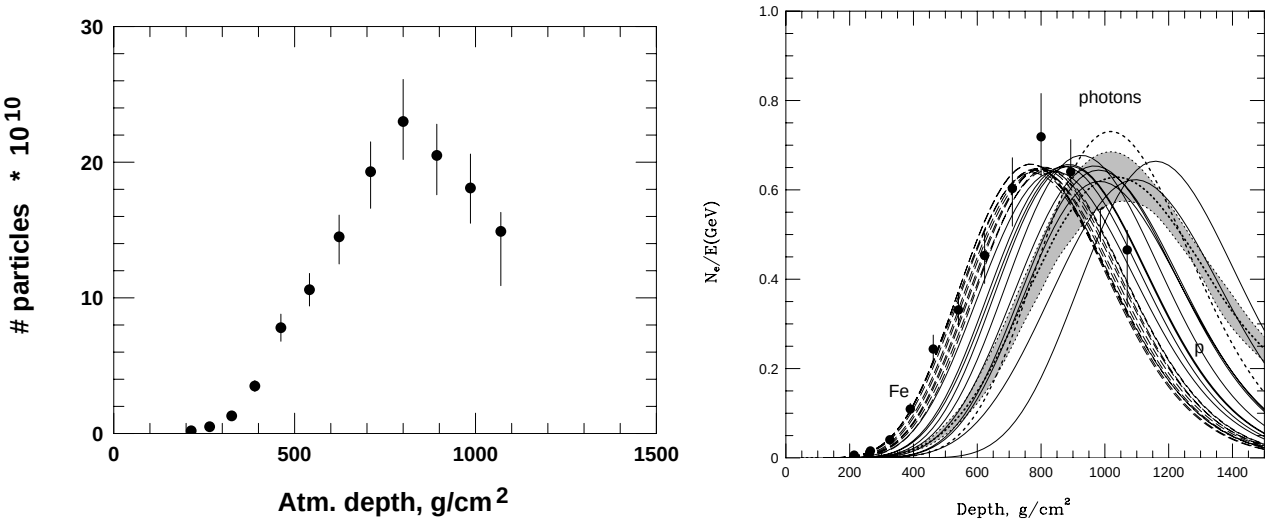

Figure 2: Left hand panel: shower profile of the highest energy cosmic ray shower detected by the Fly's Eye. Right hand panel: comparison of the detected shower profile to Monte Carlo calculations of shower initiated by protons (solid lines), iron nuclei (dashed lines), and gamma rays (shaded area, dots) in different assumptions for the development of gamma ray showers.

The errors of the estimates come from the errors of the individual data points, but mostly from the uncertainty in the distance between the detector and the shower axis. The minimum energy of about 2×10^{20} eV was calculated in the assumption that the shower axis was much closer to the detector than the data analysis derived.

It is very difficult to judge what type of the primary particle initiated the shower. A comparison of the detected shower profile with 10 showers initiated by protons and by primary iron nuclei is shown in the right hand panel of Fig. 2. It looks like the event is more consistent with the average event initiated by a light nucleus, but the fluctuations in the shower development make this notion very uncertain. On the other hand, if the same calculation

were done with some of the different hadronic interaction models, it would be fully consistent with a proton induced shower.

As we shall see later, one of the crucial questions is if the shower was initiated by a primary nucleus, or by a primary γ-ray. Fig. 2 attempts to answer this question. Gamma ray showers are usually no a subject to very big fluctuations, even after accounting for the LPM effect, which decreases the pair production cross section at very high energy. The claim from this early analysis [6] is that the detected shower profile is very different from the profiles of γ-ray showers in the corresponding energy range, and thus the primary particle if not a γ-ray.

2. ORIGIN OF UHECR

The first problem with the ultra high energy cosmic rays is that it is very difficult to imagine what their origin is. We have a standard theory for the acceleration of cosmic rays of energy below the knee of the cosmic ray spectrum at galactic supernova remnants. This suggestion was first made by Ginzburg&Syrovatskii in 1960's on the basis of energetics. The estimate was that a small fraction (3-5%) of the kinetic energy of galactic supernovae is sufficient to maintain the energy carried by the galactic cosmic rays. The acceleration process was assumed to be stochastic, Fermi type, acceleration that was later replaced with the more efficient acceleration at astrophysical shocks. See R. Blandford's lecture about different acceleration models.

This statement stands, but it is not applicable to all cosmic rays. Much more exact recent estimates and calculations show that the maximum energy achievable in acceleration on supernova remnant shocks is not much higher than 10^5 GeV. This excludes not only UHECR, but also the higher energy galactic cosmic rays, that require supernova remnants in special environments [7].

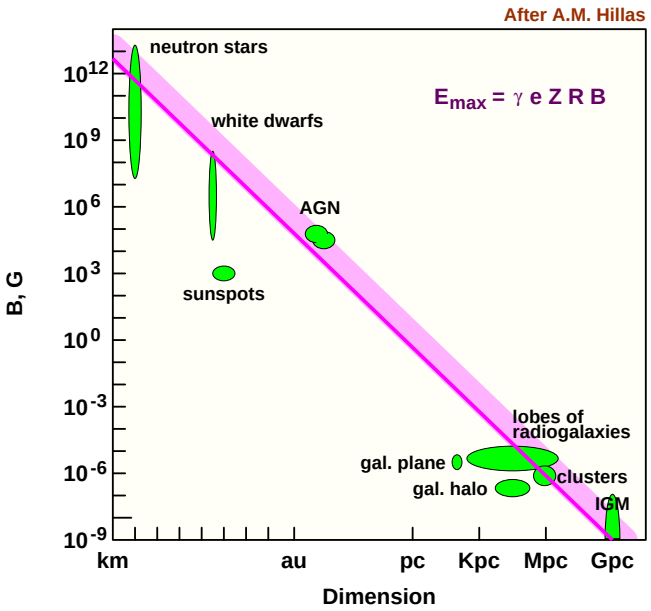

Figure 3: Requirements for acceleration of charged nuclei at astrophysical objects as spelled out by A.M. Hillas (see text).

The reader should note that currently the acceleration of charged nuclei at supernova remnants is only a theoretical prediction. Supernova remnants have higher matter density than interstellar space and one expects that the accelerated nuclei would interact with the matter and generate high energy γ-rays. Although many supernova remnants have been observed with TeV Cherenkov gamma ray telescopes, there is no proof that TeV and higher energy γ-rays are generated in hadronic interactions. We hope that the new generation of such telescopes: HESS, Magic, Kangaroo-3, and Veritas, will soon prove the prediction (see the lecture of W. Hofmann).

We should then turn to extragalactic objects for acceleration to energies exceeding 10^{20} eV. The scale for such acceleration was set up by Hillas [8] from basic dimensional arguments. The first requirement for acceleration of charged nuclei in any type of object is that the magnetic field of the object contains the accelerated nucleus within the object itself. One can thus calculate a maximum theoretical acceleration energy, that does not include and efficiency factor, as

$$E_{max} \leq \gamma e Z B R \, ,$$

where γ is the Lorentz factor of the shock matter, Z is the charge of the nucleus, B is the magnetic field value. and R is the linear dimension of the object.

Figure 3, which is a redrawn version of the original figure of Hillas, shows what are the requirements for acceleration to more than 10^{20} eV. The lower edge of the shaded area shows the minimum magnetic field value for acceleration of iron nuclei as a function of the dimension of the astrophysical object. The upper edge is for acceleration of protons.

There are very few objects that can, even before an account for efficiency, reach that energy: highly magnetized neutron stars, active galactic nuclei, lobes of giant radiogalaxies, and possibly Gpc size shocks from structure formation. Other potential acceleration sites, gamma ray bursts, are not included in the figure because of the time dependence of magnetic field and dimension.

2.1. Possible Astrophysical Sources of UHECR

In this subsection we give a brief description of some of the models for UHECR acceleration at specific astrophysical objects. For a more complete discussion one should consult a recent review paper on the astrophysical origin of UHECR [9], that contains an exhaustive list of references to particular models.

- **Pulsars:** Young magnetized neutron stars with surface magnetic fields of 10^{13} Gauss can accelerate charged iron nuclei up to energies of 10^{20} eV [10]. The acceleration process is magnetohydrodynamic, rather than stochastic as it is at astrophysical shocks. The acceleration spectrum is very flat proportional to $1/E$. It is possible that a large fraction of the observed UHECR are accelerated in our own Galaxy. There are also models for UHECR acceleration at magnetars, neutron stars with surface magnetic fields up to 10^{15} Gauss.

- **Active Galactic Nuclei:** As acceleration site of UHECR jets [11] of AGN have the advantage that acceleration on the jet frame could have maximum energy smaller than these of the observed UHECR by $1/\Gamma$, the Lorentz factor of the jet. The main problem with such models is most probably the adiabatic deceleration of the particles when the jet velocity starts slowing down.

- **Gamma Ray Bursts:** GRBs are obviously the most energetic processes that we know about. The jet Lorentz factors needed to model the GRB emission are of order 100 to 1000. These models became popular with the realization that the arrival directions of the two most energetic cosmic rays coincide with the error circles of two powerful GRB. Different theories put the acceleration site at the inner [12] or the outer [13] GRB shock. To explain the observed UHECRs with GRBs one needs fairly high current GRB activity, while most of the GRB with determined redshifts are at $Z > 1$.

- **Giant Radio Galaxies:** One of the first concrete model for UHECR acceleration is that of Rachen&Biermann, that dealt with acceleration at FR II galaxies [14]. Cosmic rays are accelerated at the 'red spots', the termination shocks of the jets that extend at more than 100 Kpc. The magnetic fields inside the red spots seem to be sufficient for acceleration up to 10^{20} eV, and the fact that these shocks are already inside the extragalactic space and there will be no adiabatic deceleration. Possible cosmologically nearby objects include Cen A (distance of 5 Mpc) and M87 in the Virgo cluster (distance of 18 Mpc).

- **Quiet Black holes:** These are very massive quiet black holes, remnants of quasars, as acceleration sites [15]. Such remnants could be located as close as 50 Mpc from our Galaxy. These objects are not active at radio frequencies, but, if massive enough, could do the job. Acceleration to 10^{20} requires a mass of 10^9 $M_\odot$.

- **Colliding Galaxies:** These systems are attractive with the numerous shocks and magnetic fields of order 20 μG that have been observed in them [16]. The sizes of the colliding galaxies are very different and with the observed high fields may exceed the gyroradius of the accelerated cosmic ray.
- **Clusters of Galaxies:** Magnetic fields of order several μG have been observed at lengthscales of 500 Kpc. Acceleration to almost 10^{20} eV is possible, but most of the lower energy cosmic rays will be contained in the cluster forever and only the highest energy particles will be able to escape [17].
- **Gpc scale shocks from structure formation:** A combination of Gpc scales with 1 nG magnetic field satisfies the Hillas criterion, however the acceleration at such shocks could be much too slow, and subject to large energy loss.

2.2. Top-Down Scenarios

Since it became obvious that the astrophysical acceleration up to 10^{20} eV and beyond is very difficult and unlikely, a large number of particle physics scenarios were discussed as explanations of the origin of UHECR. To distinguish them from the acceleration (*bottom-up*) processes they were called *top-down*. The basic idea is that very massive (GUT scale) X particles decay and the resulting fragmentation process downgrades the energy to generate the observed UHECR. Since the observed cosmic rays have energies orders of magnitude lower than the X particle mass, there are no problems with achieving the necessary energy scale. The energy content of UHECR is not very high, and the X particles do not have to be a large fraction of the dark matter.

There are two distinct branches of such theories. One of them involves the emission of X particles by topological defects. This type of models follows the early work of C.T. Hill [19] who described the emission from annihilating monopole/antimonopole pair, which forms a metastable monopolonium. The emission of massive X particles is possible by superconducting cosmic string loops as well as from cusp evaporation in normal cosmic strings and from intersecting cosmic strings. The X particles then decay in quarks and leptons. The quarks hadronize in baryons and mesons, that decay themselves along their decay chains. The end result is a number of nucleons, and much greater (about a factor of 30 in different hadronization models) and approximately equal number of γ-rays and neutrinos.

A monopole is about 40 heavier than a X particle, so every monolonium can emit 80 of them. Using that number one can estimate the number of annihilations that can provide the measured UHECR flux, which turns out to be less than 1 per year per volume such as that of the Galaxy. Another possibility is the emission of X particles from cosmic necklaces - a closed loop of cosmic string including monopoles. This particular type of topological defect has been extensively studied [20].

The other option is that the X particles themselves are remnants of the early Universe. Their lifetime should be very long, maybe longer than the age of the Universe [21]. They could also be a significant part of the cold dark matter. Being superheavy, these particle would be gravitationally attracted to the Galaxy and to the local supercluster, where their density could well exceed the average density in the Universe. There is a large number of topological defect models which are extensively reviewed in Ref. [18].

There are two main differences between bottom-up and top-down models of UHECR origin. The astrophysical acceleration generates charged nuclei, while the top-down models generate mostly neutrinos and γ-rays plus a relatively small number of protons. The energy spectrum of the cosmic rays that are generated in the decay of X particles is relatively flat, close to a power law spectrum of index α=1.5. The standard acceleration energy spectrum has index equal to or exceeding 2.

2.3. Hybrid Models

There also models that are hybrid, they include elements of both groups. The most successful of those is the Z-burst model [22, 23]. The idea is that somewhere in the Universe neutrinos of ultrahigh energy are generated. These neutrinos annihilate with cosmological neutrinos in our neighborhood and generate Z_0 bosons which decay

and generate a local flux of nucleons, pions, photons and neutrinos. The resonant energy for Z_0 production is 4×10^{21} eV/m_ν(eV), where m_ν is the mass of the cosmological neutrinos. The higher the mass of the cosmological neutrinos is, the lower the resonance energy requirement. In addition the cosmological neutrinos are gravitationally attracted to concentrations of matter and their density increases in our cosmological neighborhood. If the neutrino masses are low, then the energy of the high energy neutrinos should increase.

3. PROPAGATION OF UHECR

Particles of energy 10^{20} eV can interact on almost any target. The most common, and better known, target is the microwave background radiation (MBR). It fills the whole Universe and its number density of 400 cm^{-3} is large. The interactions on the radio and infrared backgrounds are also important. Let us have a look at the main processes that cause energy loss of nuclei and gamma rays.

3.1. Energy Loss Processes

The main energy loss process for protons is the photoproduction on astrophysical photon fields $p\gamma \to p + n\pi$. The minimum center of mass energy for photoproduction is $\sqrt{s_{thr}} = m_p + m_{\pi^0} \sim 1.08$ GeV. Since $s = m_p^2 + 2(1-\cos\theta)E_p\epsilon$ (where θ is the angle between the two particles) one can estimate the proton threshold energy for photoproduction on the MBR (average energy $\epsilon = 6.3\times10^{-4}$ eV). For $\cos\theta = 0$ the proton threshold energy is $E_{thr} = 2.3\times10^{20}$ eV. Because there are head to head collisions and because the tail of the MBR energy spectrum continues to higher energy, the intersection cross section is non zero above proton energy of 3×10^{19} eV.

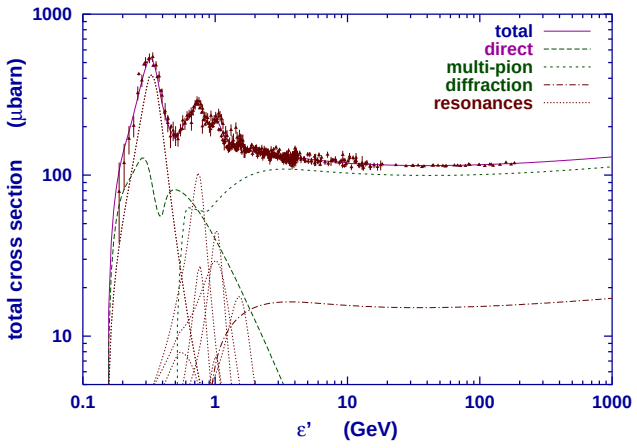

Figure 4: Photoproduction cross section as a function of the photon energy for stationary proton targets.

The photoproduction cross section is very well studied in accelerator experiments and is known in detail. Figure 3 shows the photoproduction cross section in the mirror system, as a function of the photon energy for stationary protons, i.e. as it is measured in accelerators. At threshold the most important process is the Δ^+ production where the cross section reaches a peak exceeding 500 μb. It is followed by a complicated range that includes the higher mass resonances and comes down to about 100 μb. After that one observes an increase that makes the photoproduction cross section parallel to the pp inelastic cross section. The neutron photoproduction cross section is nearly identical.

Another important parameter is the proton inelasticity k_{inel}, the fraction of its energy that a proton loses in one interaction. This quantity is energy dependent. At threshold protons lose about 18% on their energy. With increase of the CM energy this fractional energy loss increases to reach asymptotically 50%.

The proton pair production $p\gamma \to e^+e^-$ is the same process that all charged particles suffer in nuclear fields. The cross section is high, but the proton energy loss is of order $m_e/m_p \simeq 4{\times}10^{-4}$E. Figure 5 shows the energy loss length $L_{loss} = \lambda/k_{inel}$ (the ratio of the interaction length to the inelasticity coefficient) of protons in interactions in the microwave background.

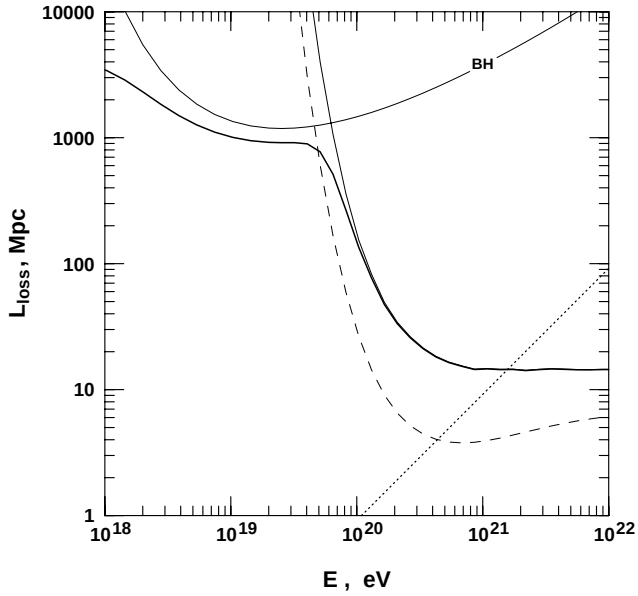

Figure 5: Energy loss length of protons in interactions in MBR.

The dashed line shows the proton interaction length and one can see the increase of k_{inel} in the ratio of the interaction to energy loss length. The contribution of the pair production is shown with a thin line. The energy loss length never exceeds 4,000 Mpc, which is the adiabatic energy loss due to the expansion of the Universe for $H_0 = 75$ km/s/Mpc. The dotted line shows the neutron decay length. Neutrons of energy less than about $3{\times}10^{20}$ eV always decay and higher energy neutrons only interact.

Heavier nuclei lose energy to a different process - photodisintegration, loss of nucleons mostly at the giant dipole resonance [25]. Since the relevant energy in the nuclear frame is of order 20 MeV, the process starts at lower energy. The resulting nuclear fragment may not be stable. It then decays and speeds up the energy loss of the whole nucleus. Ultra high energy heavy nuclei, where the energy per nucleon is higher than photoproduction, have also loss on photoproduction. The energy loss length for He nuclei in photodisintegration is as low as 10 Mpc at energy of 10^{20} eV. Heavier nuclei reach that distance at higher total energy.

UHE gamma rays also interact on the microwave background. The main process is $\gamma\gamma \to e^+e^-$. This is a resonant process and for interactions in the MBR the minimum interaction length is achieved at 10^{15} eV. The interaction length in MBR decreases at higher γ-ray energy and would be about a 50 Mpc at 10^{20} eV if not for the radio background. The radio background does exist but its number density is not well known. Figure 6 shows the interaction length for this process in MBR (dots) and in all photon fields. The energy range is wider than for protons because some top-down models can generate γ-rays of energy approaching m_X.

The fate of the electrons produced in a $\gamma\gamma$ collision depends on the strength of the magnetic fields in which UHE electrons lose energy very fast. the dashed line shows the electron energy loss length in 1 nG field. The photon energy is than quickly downgraded and the $\gamma\gamma$ interaction length becomes very close to the gamma ray energy loss length. In the case of very low magnetic fields (0.01 nG) the synchrotron energy loss is low (it is proportional to $E_e^2B^2$) and then inverse Compton scattering (with a cross section very similar to this of $\gamma\gamma$) and cascading is possible. The energy loss length of the gamma rays would be higher in such a case.

In conclusion, the energy loss of protons, heavier nuclei and photons is high in propagation on cosmological scales. Figure 7 compares the proton energy loss length to that of gamma rays in the assumption of 1 nG magnetic fields.

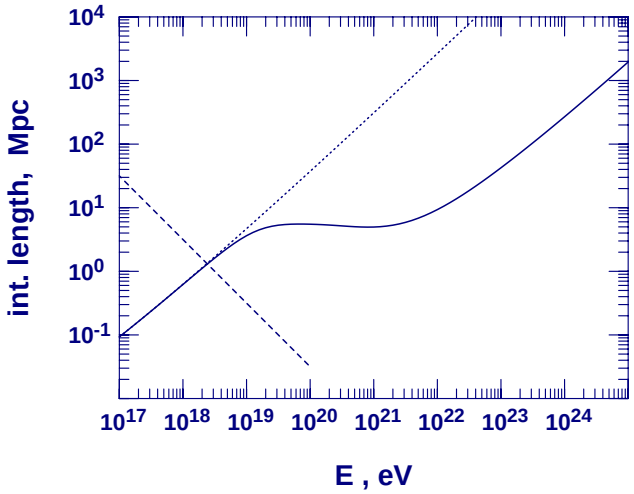

Figure 6: Interaction length of γ-rays in MBR (dots) and in MBR + radio background. The dashed line shows the synchrotron energy loss length of electrons in 1 nG magnetic field.

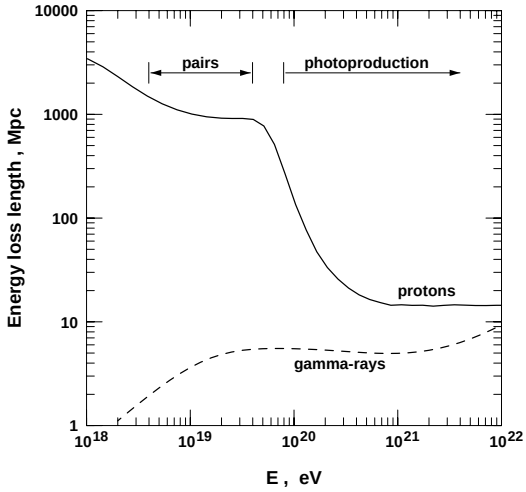

Figure 7: Energy loss lengths of protons and gamma rays,

At energies below 10^{20} eV the proton energy loss length is definitely longer than that of gamma rays. At energies above 5×10^{20} the difference is only a factor of 2, with very small energy dependence. Have in mind, though, that the flat part of the gamma ray energy loss length is due to interactions in the radio background in the 1 MHz range, which can not be detected at Earth and has to be modeled as a ratio to other astrophysical photon fields.

The general conclusion from this analysis of the energy loss of protons and gamma rays in their propagation through the Universe is these UHE particles can not survive at distances of more than few tens of Mpc and sources of the detected cosmic rays have to be located in our cosmological neighborhood. Every increase of the distance between the source and the observer would require and increase of the maximum energy at acceleration (or other production mechanism) and will increase significantly the energy requirement to the UHECR sources.

3.2. Modification of the Proton Spectrum in Propagation. Numerical Derivation of the GZK Effect.

Figure 8 shows in the left hand panel the evolution of the spectrum of protons because of energy loss during propagation at different distances. The thick solid lines shows the spectrum injected in intergalactic space by the source, which in this exercise is

$$\frac{dN}{dE} = A \times E^{-2} / \exp(E/3.16 \times 10^{21}\mathrm{eV}) \; .$$

After propagation on 10 Mpc only some of the highest energy protons are missing. This trend continues with distance and at about 40 Mpc another trend appears - the flux of protons of energy just below 10^{20} eV is above the injected one. This is the beginning of the formation of a pile-up in the range where the photoproduction cross section starts decreasing. Higher energy particles that are downgraded in this region lose energy less frequently and a pile-up is developed.

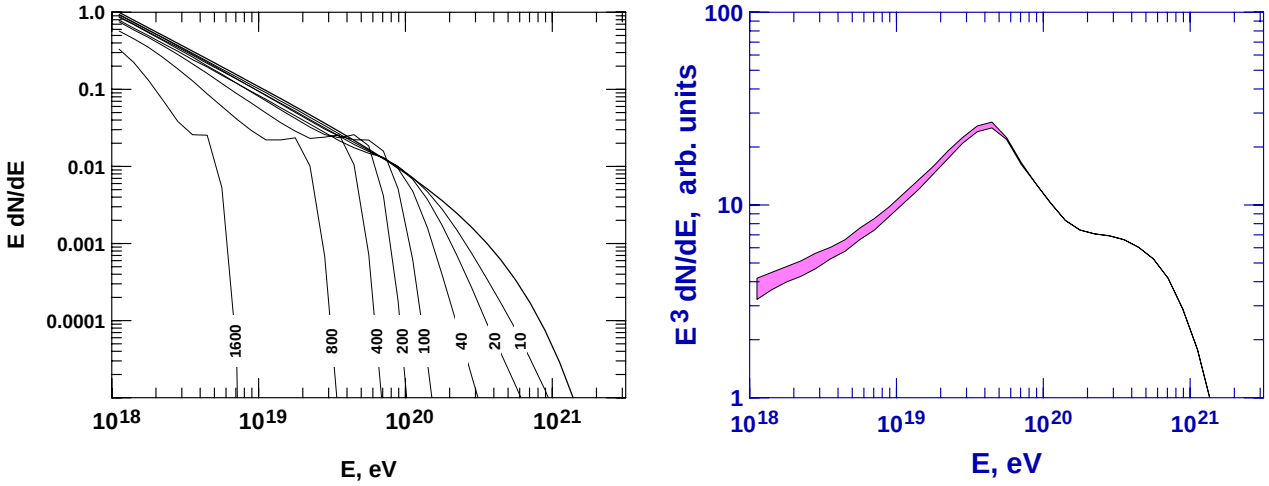

Figure 8: Left hand panel: Evolution of the cosmic ray spectrum in propagation through different distances. Right hand panel: spectrum from homogeneous isotropic cosmic ray sources that inject spectra with $\alpha = 2$. Upper edge: cosmological evolution of UHECR sources with $n = 4$, lower one - $n = 3$.

The pile-up is better visible in the spectra of protons propagated at larger distances. One should remark that the size of the pile-up depends very strongly on the shape of the injected spectrum. If it had a spectral index of 3 instead of 2 the size of the pile-up would have been barely visible as the number of high energy particles decreased by a factor of 10.

When the propagation distance exceeds 1 Gpc there are no more particles of energy above 10^{19} eV. All these particles have lost energy in photoproduction, pair production and adiabatic losses. From there on most of the losses are adiabatic.

In order to obtain the proton spectrum created by homogeneously and isotropically distributed cosmic ray sources filling the whole Universe one has to integrate a set of such (propagated) spectra in redshift using the cosmological evolution of the cosmic ray sources, which is usually assumed to be the same as that of the star forming regions (SFR) $\eta(z) = \eta(0)(1+z)^n$ with $n = 3$, or 4 up to the epoch of maximum activity z_{max} and then either constant or declining at higher redshift. High redshifts do not contribute anything to UHECR (1600 Mpc corresponds to $z = 0.4$ for $H_0 = 75$ km/s/Mpc). After accounting for the increased source activity the size of the pile-ups has a slight increase.

The right hand panel shows the UHECR spectrum that comes from the integration of propagation spectra shown in the left hand panel with different cosmological evolutions. Obviously the importance of the cosmological evolution

is very small and totally disappears for very high energy. The differential spectrum is multiplied by E^3 as is often done with experimental data to emphasize the spectral features. One can see the pile-up at 5×10^{19} eV after which the spectrum declines steeply. There is also a dip at about 10^{19} eV which is due to the energy loss on pair production. These features were first pointed at by Berezinsky & Grigorieva [26]. Such should be the energy spectrum of extragalactic protons under the assumptions of injection spectrum shape, cosmic ray luminosity (4.5×10^{44} erg/Mpc^3/yr [12]), cosmological evolution and isotropic distribution of the cosmic ray sources in the Universe.

3.3. Modification of the Gamma Ray Spectra.

Because of the strong influence of the radio background and of the cosmic magnetic fields the modification of the spectrum of gamma rays in a top-down scenario is much more difficult to calculate exactly. There are, however, many general features that are common in any of the calculations. Figure 9 shows the gamma ray spectrum emitted in a top-down scenario with $m_X = 10^{14}$ GeV [24]. The spectra of different particles from the X decay chain are indicated with different line types. The one, that we are now interested in, is for gamma rays. If not for energy loss the gamma ray spectrum would have been parallel to these of neutrinos.

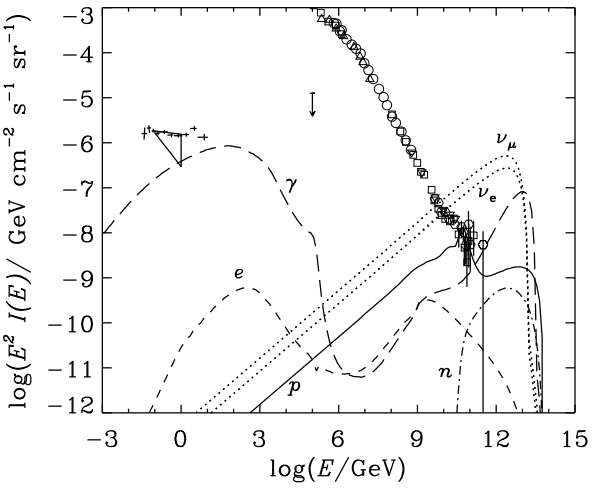

Figure 9: Evolution of the energy spectra of particles injected in a top-down scenario with X particle mass of 10^{14} GeV. The injection spectra a almost parallel to the shown neutrino spectra.

We shall start the discussion from the highest energy and follow the energy dissipation in propagation. The highest energy gamma rays have not suffered significant losses. At slightly lower energy, though, the $\gamma\gamma$ cross section grows and the energy loss increases. One can see the dip at about 10^{10-11} GeV which is caused by the radio background. All other interactions are on the MBR. The magnetic field is assumed sufficiently high that all electrons above 10^9 GeV immediately lose energy in synchrotron radiation. The minimum ration of the gamma-ray to cosmic ray flux is reached at about 10^{15} eV, after which there is some recovery. There is another absorption feature from interactions on the infrared background. The gamma ray peak in the GeV region consists mostly of synchrotron photons. Isotropic GeV gamma rays, that have been measured, can be used to restrict top-down models in some assumptions for the magnetic field strength.

3.4. UHECR Propagation and Extragalactic Magnetic Fields

The possible existence of non negligible extragalactic magnetic fields would significantly modify the propagation of the UHE cosmic rays independently of their nature and origin. There is little observational data on these fields.

The best estimate of the average strength of these fields in the Universe is 10^{-9} Gauss (1 nG) [27]. On the other hand μG fields have been observed in clusters of galaxies, and in a bridge between two parts of the Coma cluster.

Since the measurements of fields of strength less than 1 μG are very difficult, all current arguments are of strictly theoretical type. Cosmological seed fields are not expected to be stronger than 10^{-17} G. Many people believe that the Universe is much too young to explain the existence of significant large scale fields by spreding out the fields of individual astrophysical objects. Others are impressed by the high fields observed in clusters of galaxies and suspect the existence of lower fields on larger scales.

No one expects the extragalactic magnetic fields to be isotropic. They should be much higher than the average is the walls of high matter density and much lower in the voids. All possible UHECR sources should also be associated with high matter concentration.

Even fields with nG strength would seriously affect the propagation of UHE cosmic rays. If UHECR are protons they would scatter of these fields. This scattering would lead to deviations from the source direction and to an increase of the pathlength from the source to the observer. It would make the source directions less obvious and would create a magnetic horizon for extragalactic protons of energy below 10^{19} eV as their propagation time from the source to the observer would start exceeding Hubble time.

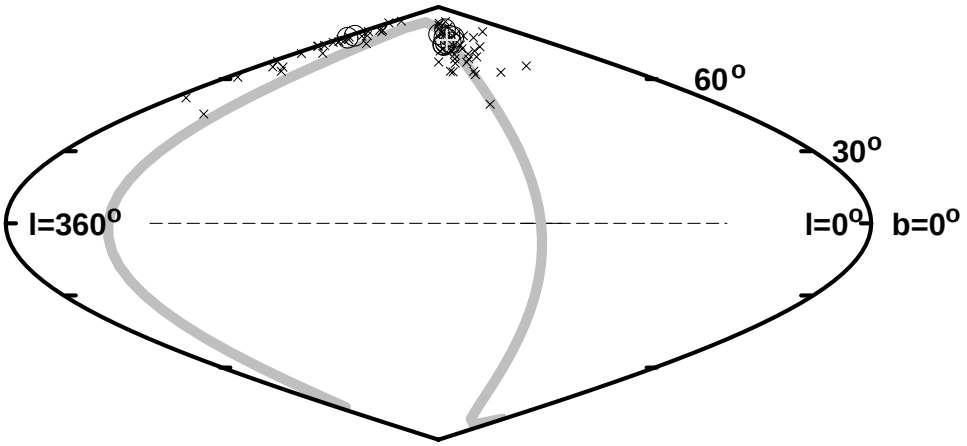

Figure 10: The arrival direction in galactic coordinates of protons emitted by M87 (cross) if there were an organized 10 nG field along the Supergalactic plane (shown with wide gray curve). Particles above 10^{20} eV are shown with circles. The Galactic plane is indicated with a dashed line. The map is centered at the Galactic anticenter.

If regular magnetic fields of strength exceeding 10 nG were present on 10 Mpc coherence length they would lead to significant biases in the propagated spectra [28] in a function of the relative geometry of the field, source and observer. Particles of very high energy would gyrate around the magnetic field lines and thus appear coming from a wide range of directions. Figure 10 shows an example for protons accelerated at the powerful AGN M87 in case is connected with our galaxy by 3 Mpc wide cylinder of 10 nG magnetic field. The distance to M87 is 18 Mpc. If such fields indeed exist, one should be able to recognize the UHECR sources only on the basis of high statistics.

The strongest possible magnetic field effect on UHE cosmic ray nuclei was suggested by Biermann [29]. He used the observational fact that in all observed spiral galaxies the magnetic field is directed inward along the spiral arms and applied Parker's solar field model to obtain a model of the galactic wind. Galactic magnetic fields are frozen in the galactic wind. Protons of energy 10^{20} eV can penetrate the resulting magnetic bottle only from the galactic North and the most likely origin of the detected UHECR is then in the vicinity of the Virgo cluster.

The influence of magnetic fields on gamma ray propagation is mostly restricted to the rate of energy loss in propagation. Fig. 6 shows with a dotted line the synchrotron energy loss of electrons in 1 nG magnetic field. In the absence of magnetic fields electrons would have inverse Compton interactions on MBR that would generate a gamma ray that carries almost the total electron energy. This would lead to electromagnetic cascading and relatively slow decrease of the γ-ray energy. In the presence of fields the electrons of energy above 3×10^{18} eV would lose energy

very fast on synchrotron radiation. The radiated photons would have energies lower by many orders of magnitude. This is one of the bases for limiting the allowed mass of the X particles in the exotic particle physics models of the UHECR origin.

3.5. Production of Secondary Particles in Propagation

One interesting feature that can be used for testing of the type and distribution of UHECR sources, that we shall not discuss at any length, is the production of secondary particles in propagation. The energy loss of the primary protons and γ-rays is converted to secondary gamma rays and neutrinos.

Most interesting are the cosmogenic neutrinos, that were first proposed by Berezinsky & Zatsepin [30] and have been since calculated many times, most recently in Ref. [31]. Every charged pion produced in a photoproduction interaction three neutrinos through its decay chain.

The spectrum of cosmogenic neutrinos depends on the UHECR spectrum and on the UHECR source distribution. It extends to energies exceeding 10^{20} eV. Currently designed and built neutrino telescopes are aiming at detection of cosmological neutrinos (see P. Gorham's talk).

At the Δ resonance energy range 2/3 of the produced pions are neutral. Most of the energy loss (including those in e^+e^- pairs) goes to the electromagnetic component as do the muon decay electrons. The ensuing electromagnetic cascading should create a γ-ray halo around powerful UHECR sources that could be detected by the new generation of γ-ray detectors.

3.6. Particle Physics Models

There are also quite a few models that attempt to avoid the propagation difficultios by assuming that UHECR are not any of the known stable particles. One of these models [32, 33] assumes that the gluino is the lightest supersymmetric particle and that it causes the observed UHE cosmic ray showers. It gluinos have mass between 0.1 and 1 GeV, it could have photoproduction cross section much smaller than that ot nucleons and still be able to interact in the atmosphere and generate showers. The distance to potential gluino sources could reach many hundreds of Mpc. The problems with this and other similar models that neutron particles can not be accelerated and gluinos have to be copiously produced at the source in interactions of particles of still higher energy. So the problems again lead to the mechanisms of particle acceleration well above 10^{20} eV.

Starting with Refs. [34, 35] many authors have discussed different effects that could help propagate protons and much larger distances than calculated above. The original suggestions are for tiny violations of the Lorentz invariance that can not be detected in any other way. Coleman & Glashow define a maximum achievable velocity (MAV) for the particles involved in photoproduction interactions that are due to Lorentz invariance violations. Small (order of 10^{-23} differences between proton and Δ^+ or proton and pion MAV would increase the photoproduction threshold and thus significantly increase the energy of the GZK cutoff.

4. EXPERIMENTAL DATA

There are six experiments that have collected experimental data after the Volcano Ranch array that Linsley ran. SUGAR, Haverah Park, Yakutsk, and AGASA are surface air shower arrays. Fly's Eye and its successor HiRes are fluorescent detectors. The current world statistics on UHECR are dominated by AGASA and HiRes. These two experiments have presented data on the energy spectrum, some shower features (X_{max}) and arrival direction distributions for their data samples. The statistics is still quite small and the main results of the two detectors are somewhat in contradiction.

4.1. Energy Spectra of UHECR

Figure 11 shows in the left hand panel the UHECR spectra measured by AGASA [36] and by HiRes [37, 38] in monocular mode. This experiment is designed to look for showers *in stereo*, with two optical detectors that observe the shower simultaneously. The shower analysis is much easier and exact in such a mode. The data shown in Fig. 11 are taken by the two optical detectors independently. The experimental statistics of HiRes in stereo is still smaller.

There two facts that one immediately notices:

1) The overall normalization of the cosmic ray flux is different by about 40%, which looks like a factor of 2 in the figure because of the E^3 factor on the differential flux.

2) AGASA sees eleven showers with energy above 10^{20} eV. HiRes sees only two with a an exposure that is estimated twice the AGASA's.

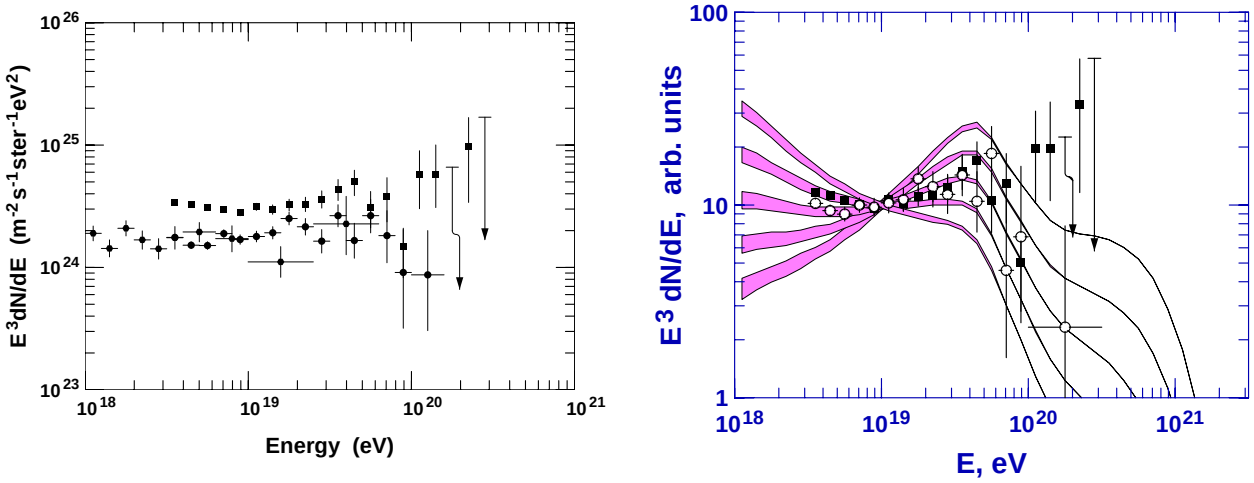

Figure 11: Left hand panel: the experimental data of AGASA (full squares) and of HiRes in monocular mode (dots). Right hand panel: The data are normalized to each other at 10^{19} eV and are compared in shape to calculations such as shown in Fig. 8 with injection spectra with indices of 2.00, 2.25, 2.50, 2.75, and 3.00 (bottom to top at 10^{18} eV.

The energy assignment of the AGASA experiment is done by the particle density at 600 meters from the core (ρ_{600}) which is not very sensitive to the type of the primary nucleus. HiRes estimates the primary energy either by the integral of the shower profile. Both experiments claim systematic uncertainties of order 30%.

The data from the other experiments are intermediate between these two extremes. Each experiment has seen at least one event that has energy well above 10^{20} eV, but with small experimental statistics the flux of such events is very uncertain.

When the difference in flux normalization (which could well be a difference in energy assignment) is taken out, the spectral shapes are not that different, as shown in the right hand panel of Fig. 11. The spectra agree in shape quite well up to 10^{20} eV. They may show a dip at about $10^{19.7}$ eV. The big difference is that the AGASA spectrum recovers and that of HiRes does not. Because of the small statistics the difference between the two data sets at the highest energies is not statistically significant [39].

Another question that Fig. 11 raises is on the UHECR injection spectrum. The eyes (and numerous fits) prefer a spectral index in the vicinity of 2.50 in the case of homogeneous isotropic source distribution. Flatter injection spectra could be fitted only by a strong contribution of the galactic cosmic rays up to 10^{19} eV. Distinguishing between galactic and extragalactic contribution would only be possible if the chemical composition of UHECR is known - galactic cosmic rays at this energy have to be heavy nuclei.

Another difference between the two measurements, which is not that easy to see, is that they observe the ankle at different energy: about 3×10^{18} eV by HiRes and about 10^{19} eV by AGASA. This is obviously not related to the energy assignments discussed above, which only differ by 40% or so.

4.2. Chemical Composition of UHECR

The predecessor of HiRes, the Fly's Eye, studied the UHECR composition by fitting the energy dependence of the depth of maximum X_{max} of the UHE air showers. In electromagnetic showers X_{max} is proportional to logarithm of the primary energy $\ln E$. In showers initiated by primary nuclei this dependence is a more complicated function of the energy, but is still proportional to the primary energy per nucleon. Because of that X_{max} of an iron initiated shower of energy E_0 would be approximately the same as of a proton shower of energy $E_0/56$.

The change of X_{max} in one decade of E_0 was called elongation rate (ER) by John Linsley. Contemporary hadronic interaction models predict elongation rate of 50 to 60 g/cm^2. The Fly's Eye observed an ER of more than 70 g/cm^2 to energies 3×10^{17} eV followed by a change that made the elongation rate consistent with expectations [40]. The Fly's Eye thus observed a simultaneous change of the slope of the cosmic ray spectrum and of the shower elongation rate [41].

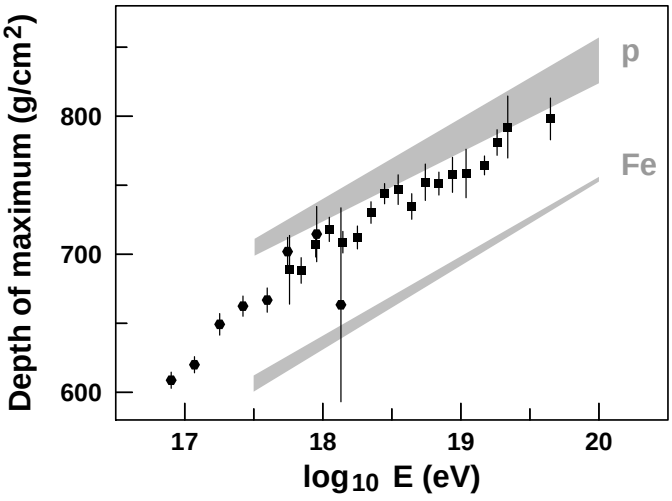

Figure 12: Depth of maximum as a function of the shower energy, as measured by HiRes (squares) and HiRes prototype + CASA/MIA (hexagons). The shaded areas are the predictions of different hadronic interaction models.

This is an enormously important statement, because it implies that the the mass of the primary cosmic rays is becoming lighter. It signals that the flux of heavy galactic cosmic rays is decreasing and the new cosmic ray component that is responsible for the change of the spectral index at the ankle consists of protons and possibly He nuclei.

This observation is now supported [42] by the new results of HiRes shown in Fig. 12. The lower energy points shown with hexagons are obtained with the HiRes prototype working together with CASA/MIA air shower array. According to this most recent data set the change of the cosmic ray composition is almost over by 10^{18} eV. Since the observed X_{max} is almost parallel to the expectations, one can assume that the composition is constant. The composition is proton dominated, but a more exact prediction depends on the hadronic interaction model used, as shown with shaded areas that indicate calculations with different hadronic models.

The chemical composition of the primary cosmic rays can also be studied by the fraction of muons in the showers. When the primary particle is a heavy nucleus, the first generation mesons are approximately 1/A less energetic than in protons showers, and have a higher decay probability. For this reason the muon fractions is higher in showers generated by heavy nuclei. The AGASA experiment has a number of muon counters that can study the muon content of the showers. The number of such counters is not high and the statistics is thus limited, but the AGASA collaboration did not see the change in the muon content that would correspond the the Fly's Eye result. The collaboration still claims a gradual decrease of the Fe fraction between energies of $10^{17.5}$ and 10^{19} eV. Alternative methods for estimation of the cosmic ray composition, applied by other experimental groups, also give a relatively

large fraction of heavy nuclei around 10^{18} eV.

This disagreement is still not fully solved. The showers of both groups are now analyzed using the same hadronic interaction models but the differences persist.

Especially important is the determination of the type of the UHECR - nuclei or gamma rays. Two special studies have been performed by the AGASA and the Haverah Park groups using different approaches. AGASA [43] looks at the particle density at 100 meters from the shower core that is expected to be dominated by shower muons. This density should be much lower in gamma ray initiated showers. A new analysis of the Haverah Park data [44] studies highly inclined air showers. Since the absorption of gamma ray showers is stronger, their flux should decline with zenith angle faster. Both experiments limit the fraction of γ-rays above 10^{19} eV at 30% of all cosmic rays. The limits at higher energy (3-4$\times 10^{19}$ eV) are less strict(67% - 55%) because of the declining statistics. There is no statement about the few particles above 10^{20} eV so that 'top-down' models can still apply to these events.

4.3. Arrival Directions of UHECR

The arrival direction distribution of the UHECR events detected by AGASA has two main features: the distribution is isotropic on large scale and non isotropic on small (one degree) scale [45]. There is no preference of higher event rate coming from the galactic plane or any other know astrophysical concentration of matter, although an association with the supergallactic plane was reported [46] on the basis of an earlier smaller event sample. There are however five doublets and a triplet of events arriving at less than 2.5° from each other. The angular resolution of the detector is below 2°. The statistical significance of this 'clustering' is of order three σ. The individual clusters can be identified in Fig. 13 that shows the arrival directions of the world data set above $10^{19.6}$ eV, except for the Fly's Eye and HiRes events that are not yet published.

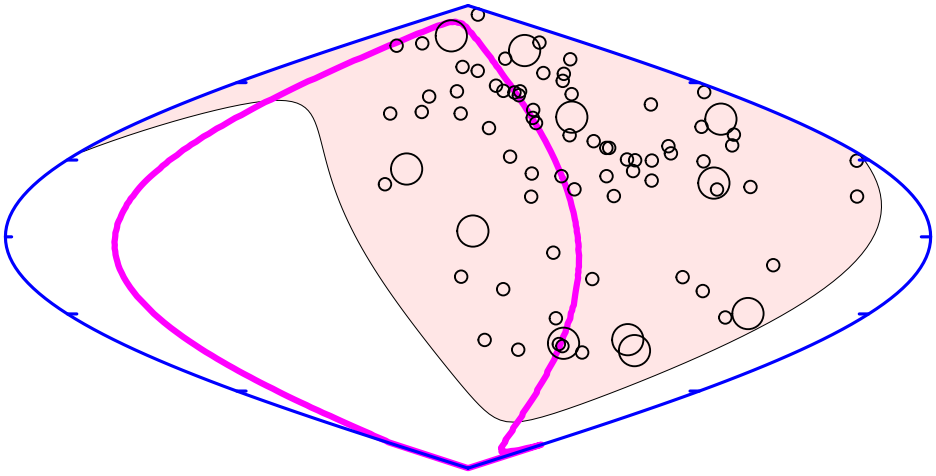

Figure 13: Arrival directions of cosmic rays of energy exceeding $10^{19.6}$ eV in galactic coordinates. The map is centered on the galactic anti-center. The large circles identify energies exceeding 10^{20} eV. The shaded area is the field of view of the detectors. The thick line indicates the supergalactic plane - the plane of weight of galaxies at redshifts less than 0.04.

The clusters do not point at any known luminous astrophysical object. There have been long discussions how such clustering can occur in a more or less realistic astrophysical scenario. Do they point at UHECR sources that we cannot otherwise observe? How many UHECR sources should exist to fit both the isotropic large scale distribution and the clustering? Is the clustering real, or a result of a large statistical fluctuation?

One of the better ways to look at the small scale anisotropy of the AGASA showers is to look at the self-correlation of the detected showers. Fig. 14 shows the self-correlation plot - the number of events that have directions different from each other by $\Delta\alpha$. The real number of events is divided by the expectation from isotropic distribution and is given in the figure in terms of σ. The clustering is at $\Delta\alpha$ less than 2°, which would correspond to the angular

resolution of the detector. The statistical significance reaches 5σ, significantly higher than simply counting the number of clusters.

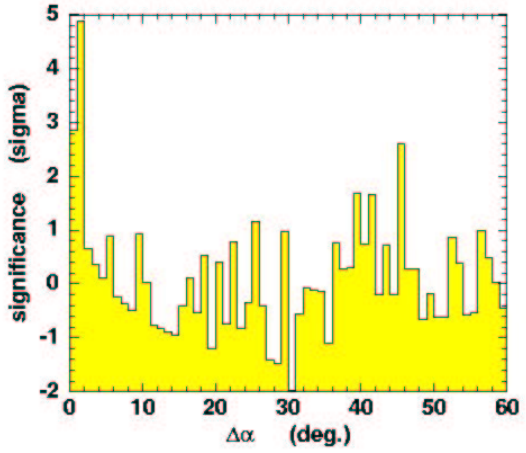

Figure 14: Self correlation plot of the arrival directions of the AGASA showers of energy above 4×10^{19} eV.

Unfortunately there is again a controversy between the observations with the highest statistics - the HiRes collaboration does not confirm [47] the clustering of events reported by AGASA. The much more accurate stereoscopic event reconstruction does not find [48] small scale anisotropy. It is difficult to compare directly the results of the two groups because the HiRes event sample above 10^{19} eV is smaller. HiRes, however, claims that there is no statistically significant anisotropies on angular scales up tp 5° at any energy threshold above 10^{19} eV.

A detailed review of the experimental approaches and data before the most recent HiRes publications is this of Nagano $ Watson [49] The main qualitative and contradictory experimental results obtained by the current experiments with the highest statistics are summarized below.

	AGASA	HiRes
are there super GZK events	many	a few
have we observed GZK cutoff	yes	no
is there large scale isotropy	yes	yes
is there small scale isotropy	no	yes
UHECR composition changing at	3×10^{18} eV	10^{18} eV

We were nevertheless able to estimate, although very roughly, the main astrophysical parameters related to ultra high energy cosmic rays. The emissivity of particles of energy between 10^{19} and 10^{21} derived for $\alpha = 2$ injection spectra [12] is 4.5×10^{44} ergs/Mpc^3/yr. For injection spectra of index 2.7 the emissivity in the same units is above 10^{46} [50]. There is a strong dependence of the emissivity at all energies on the steepness of the injection spectrum and on the *minimum* of the energy spectrum at acceleration.

The density of the UHECR sources has been estimated from the clustering of the AGASA cosmic rays events [51–53] to $10^{-5\pm1}$ Mpc^{-3} depending on the assumptions for the extragalactic magnetic fields.

The energy spectrum detected by AGASA can be explained by a combination of isotropic homogeneous UHECR source distribution, galactic cosmic rays and local UHECR sources or top-down scenarios. The HiRes spectrum does not require local sources or top-down models.

We have yet no idea what the cosmological evolution of the UHECR sources is. Steep injection spectra do not require any cosmological evolution. Flat injection spectra do.

5. FUTURE OF THE FIELD

It is obvious that at least a part of the inconsistency of the current experimental results is due to the very low experimental statistics. The interest in UHECR actually grew when ideas for experiments that can solve the problem appeared in the early 1990s. Obviously shower arrays much bigger than AGASA are needed when the aim is to collect reasonable statistics above 10^{20} eV. The first idea for the Auger Observatory [54] was spelled out by Cronin & Watson.

Auger would initially consist of two air shower arrays located in the Northern and in the Southern hemispheres, each of area 5,000 km^2, i.e. it was supposed to be 100 times the size of AGASA. Arrays in both hemispheres are needed for full sky coverage - nobody knows where the UHECR sources are. This first proposal is scaled down, but the Southern Auger Observatory is being built in Argentina (see talk of R. Cintra Shellard). It consists of 3,000 km^2 area observed by surface detectors and by four fluorescent detectors. The surface detectors are 10 m^2 water Cherenkov tanks spaced by 1,500 m. One meter tall water Cherenkov tanks were chosen because they absorb almost fully all shower electrons and photons and because their area does not decrease that fast with zenith angle - they will be able to observe and reconstruct showers down to horizontal direction. Another big advantage is that about 10% of the statistics will be observed simultaneously with both techniques, which may solve the current contradictions of AGASA and HiRes.

Then there is the Telescope Array (TA) [55] that is already funded by the Japanese government. TA will consist of 1,000 km^2 surface array equipped with scintillator detectors 1.2 km apart from each other and three fluorescent detectors observing the atmosphere above it. There are plans for moving the HiRes detectors to TA and infilling the ground array to extend the threshold to lower energy. The latter part is not yet funded.

Other, longer time scale, plans are for space based giant air shower detectors. EUSO [56] was chosen by the European Space Agency as a Phase A project to be mounted on the International Space Station. EUSO is a fluorescence detector that observes the atmosphere from an altitude of 400 km. It will be able to cover more than 10^5 km^2 with a resolution about 1 km per pixel. Such a detector will be very efficient for observation of highly inclined showers, and thus it would be a very good detector of UHE neutrinos that would interact very deep in the atmosphere. EUSO was not approved for Phase B because of the uncertainty of the ISS future, but the design of the detector and the necessary measurements of the relevant atmospheric features are still funded and continue.

OWL [57] is an even more ambitious project for stereoscopic observations from space with two detectors mounted on free flying satellites. These satellites would see the Earth from higher altitude, and thus observe larger area. The stereoscopic observation will make the analysis of the detected events easier and more exact. OWL is a part of the NASA plans for the future.

6. SUMMARY

We are certain that cosmic rays of energy above 10^{20} eV exist, but their flux is unknown. All giant air showers arrays have detected at least one shower of energy above 10^{20} eV. The puzzle is that very few astrophysical objects can accelerate charged nuclei to such energy in shock acceleration processes, which is the favorite model for astrophysical acceleration.

Protons and heavier nuclei lose energy in propagation in photoproduction and photodisintegration on MBR and other photon fields. Since the energy loss length of all nuclei is of order 10 Mpc, the UHECR sources have to be within tens of Mpc from our Galaxy. There are few powerful astrophysical objects that close to us.

The other possibility are 'top-down' scenarios where these particles are generated in the decay of ultraheavy X-particles, which could be emitted by cosmic strings or are long lived remnants of the early Universe.

The current experimental data are not able to give us good indication on the type of these UHECR and their arrival direction distributions. The data on the cosmic ray spectrum and composition above 10^{18} eV are somewhat contradictory. The HiRes experiment gives UHECR spectrum and composition fully consistent with the assumption of isotropic distribution of the cosmic rays sources. The HiRes predecessor, Fly's Eye, has detected the highest energy

event of energy 3×10^{20} eV. The AGASA experiment has published several events of super GZK energy which show no cutoff in the UHE cosmic ray spectrum. AGASA also claims a small scale anisotropy of the events above 10^{19} eV which is not, however, related to the directions of powerful astrophysical objects.

New third (and fourth) giant air shower experiments are being designed and built. They will increase the world data sample by orders of magnitude and help understanding the nature and sources of these exceptional events.

Acknowledgments

My work in the field of UHECR is funded in part by U.S. Department of energy contract DE-FG02 91ER 40626 and by NASA grant NAG5-7009. The collaboration of J. Alvarez-Muñiz, P.L.Biermann, R. Engel, T.K. Gaisser, D. Seckel and others is highly appreciated.

References

[1] J. Linsley, Phys. Rev. Lett., **10**, 146 (1963)
[2] G. Cocconi, Nuovo Cimento, **3**, 1422 (1956)
[3] K. Greisen, Phys. Rev. Lett. **16**, 748 (1966)
[4] G.T. Zatsepin & V.A. Kuzmin, JETP Lett. **4** 78 (1966).
[5] D.J. Bird et al., Phys. Rev. Lett., **71**, 3401 (1993)
[6] F. Halzen et al., Astropart. Phys., **3**, 151 (1995)
[7] H. Völk & P.L. Biermann,
[8] A.M. Hillas, Ann. Rev. Astron. Astrophys., **22**, 425 (1984)
[9] D.F. Torres & L.A. Anchordoqui, Rep. Prog. Phys., **67**, 1663 (2004)
[10] P. Blasi, R.I. Epstein & A.V. Olinto, Ap.J., **533**, L33 (2000)
[11] F. Halzen & E. Zas, Ap. J., **488**, 607 (1997)
[12] E. Waxman, Ap. J., **452** 1 (1995)
[13] M. Vietri, Ap. J., **453**, 883 (1995)
[14] J.P. Rachen & P.L. Biermann, A&A, **272**, 161 (1993)
[15] E. Boldt & P. Ghosh, MNRAS, **307**, 491 (1999)
[16] C.J. Cesarsky, Nucl. Phys. B (Proc. Suppl.), **28**, 51 (1992)
[17] H. Kang, D. Ryu & T.W. Jones, Ap. J., **456**, 422 (1998).
[18] P. Bhattacharjee & G. Sigl, Phys. Reports, **327**, 109 (2000)
[19] C.T. Hill, Nucl. Phys., b**224**, 469 (1983)
[20] V.S. Berezinsky& A. Vilenkin, Phys. Rev. Lett., **79**, 5202 (1997)
[21] V.S. Berezinsky, M. Kahelriess & A. Vilenkin, Phys. Rev. Lett., **79**, 4302 (1997)
[22] T.J. Weiler, Astropart. Phys., **11**, 303 (1999)
[23] D. Fargion, B. Mele & A. Salis, Ap. J., **517**, 725 (1999)
[24] R.J. Protheroe and T. Stanev, Phys. Rev. Letters, **77**, 3708 (1996)
[25] J.L. Puget, F.W. Stecker & J.H. Bredekamp, Ap. J., **205**, 538 (1976)
[26] V.S. Berezinsky & S.I. Grigorieva, A&A, **199**, 1 (1988)
[27] P.P. Kronberg, Rep. Progr. Phys., **57**, 325 (1994)
[28] T. Stanev, D. Seckel & R. Engel, Phys. Rev. D, **68**:103004 (2003)
[29] P.L. Biermann et al., Nucl. Phys. B (Proc. Suppl), **87**, 417 (2000)
[30] V.S. Berezinsky & G.T. Zatsepin, Phys. Lett. **28b**, 423 (1969); Sov. J. Nucl. Phys. **11**, 111 (1970).
[31] R. Engel, D. Seckel & T. Stanev, Phys. Rev. D64:09310 (2001)
[32] G. Farrar, Phys.Rev. Lett., **76**, 4111 (1996)
[33] G. Farrar & P.L. Biermann, Phys. Rev. Lett., **81**, 3579 (1998)

[34] L. Gonzalez-Mestres, Nucl. Phys. B (Proc. Suppl.), **48**, 131 (1996)
[35] S. Coleman & S.L. Glashow, Phys. Lett., B**405**, 219 (1997); Phys. Rev. D**59**:116008 (1999)
[36] M. Takeda et al., Phys. Rev. Lett., **81**, 1163 (1998); for updates see `http://www-akeno.icrr.u-tokio.ac.jp`
[37] R.U. Abbasi et al. (HiRes Collaboration), Phys. Rev. Lett., **92:** 151101 (2004)
[38] T. Abu-Zayyad et al.(HiRes Collaboration), astro-ph/0208301
[39] D. De Marco, P. Blasi & A.V. Olinto, Astropart.Phys., **20**, 53 (2003)2003
[40] T.K. Gaisser et al. (HiRes Collaboration) Phys. Rev. D**47**, 1919 (1993)
[41] D.J. Bird et al., Phys. Rev. Lett. 71, 3401 (1993)
[42] R.U. Abbasi et al. (HiRes Collaboration) astro-ph/0407622
[43] K. Shinozaki et al, Ap. J., **571**. L117 (2002)
[44] M. Ave et al, Phys. Rev. Lett., 85, 2244 (2000)
[45] Y. Uchihori et al., Astropart. Phys., **13**, 151 (2000)
[46] T. Stanev et al., Phys. Rev. Lett. **75**, 3056 (1995)
[47] R.U. Abbasi et al. (HiRes Collaboration), Astropart. Phys., **22**, 139 (2004)
[48] R.U. Abbasi et al. (HiRes Collaboration), Ap. J., **610**, L73 (2004)
[49] M. Nagano & A.A. Watson, Rev. Mod. Phys. **72**, 689 (2000)
[50] V.S. Berezinsky, A.Z. Gazizov & S.I. Grigorieva, astro-ph/0204357
[51] P. Blasi & D. De Marco, Astropart. Phys., **20**, 559 (2004)
[52] G. Sigl, F. Miniati & T.A. Ensslin, Phys. Rev. D**70:**043007 (2004)
[53] H. Yoshiguchi, S. Nagataki & K. Sato, Ap. J., **592**, 311 (2003)
[54] *http://www.auger.org*
[55] *http://www-ta. icrr.u-tokyo.ac.jp*
[56] *http://www.euso-mission.org*
[57] *http://owl.gsfc.nasa.gov*